ORIGINAL ARTICLE

Corrosion Studies of $Hf_{64}Cu_{18}Ni_{18}$ Metallic Glass in Acidic and Alkaline Media

Anuj Khond[1] · Shashi B. Arya[2] · Bhaskar Majumdar[3] · Jatin Bhatt[1] · Ajeet K. Srivastav[1]

Abstract In the present paper, the corrosion behavior of Hf-rich $Hf_{64}Cu_{18}Ni_{18}$ (at%) metallic glass (MG) was studied in acidic and alkaline media using electrochemical polarization experiments. Three different molar solutions of NaOH and HCl were used for the experiments. The results show that the glassy alloy possesses significantly high corrosion resistance in alkaline solution than acidic one. Pits are observed on the sample in acidic media, whereas alkaline sample does not show pitting. In both the solutions, primarily, HfO_2 is formed on the surface as a corrosion product. The corroded surface is non-uniformly distributed on the ribbon and found to decrease with concentration of NaOH. The non-uniform distribution is attributed to inhomogeneity in the ribbon sample. In case of HCl solution, corroded surface increases with the increase in HCl concentration. Furthermore, an attempt has been made to understand the corrosion mechanism of this MG in view of phases formed during the experiment.

Keywords Metallic glass · Corrosion resistance · Pitting corrosion · Passivity

✉ Anuj Khond
anujkhond22@gmail.com

1   Department of Metallurgical and Materials Engineering, Visvesvaraya National Institute of Technology, Nagpur 440010, India

2   Department of Metallurgical and Materials Engineering, National Institute of Technology Karnataka, Surathkal 575025, India

3   Defence Metallurgical Research Laboratory, Kanchanbagh, Hyderabad 500058, India

1 Introduction

Metallic glasses (MGs) are emerging as excellent materials for engineering and technological applications in the recent past [1]. Owing to the absence of a crystalline lattice and defects such as dislocations and grain boundary, metallic glasses possess a unique deformation mechanism [2]. Deformation mechanism is governed by initiation and propagation of shear band rather than dislocation movements [3, 4]. Due to this feature metallic glasses exhibit high strength, high hardness, good wear resistance, and large elastic deformation. So, the improved mechanical properties lead to metallic glasses as excellent materials for engineering and technological applications. In addition to this Fe-, Zr-, Co-, and Ti-based bulk glassy alloys have significantly being used in functional system such as rotation magnetic sensors, micro-geared motors, pressure sensors, optical devices, Colliori-type mass flow meters, high corrosion-resistant surface coating layers, shot peening balls, fixation devices for bone and teeth, and electromagnetic materials [5]. In addition, it is well known that the amorphous structure has better corrosion resistance than the crystalline counterpart due to lack of defects like dislocation and grain boundaries, and the presence of chemical homogeneity of single-phase amorphous alloy [6]. However, MGs are required to be more chemically stable against aggressive environments [7, 8], and therefore, the corrosion properties of these materials are one of the primary concerns in different corrosive media. The aggressive corrosive media ultimately lead to the deterioration of material despite their favorable mechanical properties [9]. Corrosion studies have been reported so far on various MGs in different corrosive media such as sodium chloride (NaCl), hydrochloric acid (HCl), sodium hydroxide (NaOH), and sulfuric acid (H_2SO_4) [10].

In view of the above-mentioned points, high corrosion resistance is one of the essential requirements to diversify the application of MGs. Until now, corrosion studies of well-established Zr- [9, 11], Cr- [12], Cu- [13, 14], Mg-[15–17], Ti- [18], and Fe- [19, 20] based bulk metallic glasses have been reported in different corrosive media depending upon the application. The corrosion behavior of Hafnium (Hf)-rich metallic glasses has not been analyzed, so far. Hence, an Hf-rich metallic glass was chosen for the corrosion studies in the present work. Li et al.[21], Louzguine et al. [22], and Zhang et al. [23] have synthesized Hf-Cu-Ni MG. Moreover, Cui et al. [24] have proposed MG forming composition in the Hf-Cu-Ni system by molecular dynamics (MD) simulation. In our previous research work [25], the Hf-Cu-Ni MG synthesis was reported after optimizing the glass-forming composition by thermodynamic modeling. We synthesized four different Hf-based metallic glasses, namely $Hf_{57}Cu_{11}Ni_{32}$, $Hf_{59}Cu_{18}Ni_{23}$, $Hf_{60}Cu_{21}Ni_{19}$, and $Hf_{64}Cu_{18}Ni_{18}$ by rapid solidification processing. Out of these four, maximum Hf content glass ($Hf_{64}Cu_{18}Ni_{18}$) was selected for the corrosion studies.

Typically from an application point of view, MGs are subjected to two conventional corrosive media, i.e., alkaline and acidic [26]. Alkaline media consist of NaOH, KOH, $Mg(OH)_2$, and $CaCO_3$ whereas acidic media consist of HCl and H_2SO_4. Hydroxides and chloride containing media are the conventional electrolytes used by the BMGs research community [26]. In view of this in the present work, an experimental case study has been performed to understand the corrosion behavior of $Hf_{64}Cu_{18}Ni_{18}$ MG in alkaline and acidic media with varying concentration in NaOH and HCl solutions.

2 Experimental Details

Hf-based ($Hf_{64}Cu_{18}Ni_{18}$) metallic glass (MG) ribbon was synthesized by rapid solidification processing. The X-ray diffraction (XRD) study of metallic glass showed the glassy nature of $Hf_{64}Cu_{18}Ni_{18}$ MG [25]. Temperature values such as glass transition (T_g), crystallization (T_x), and melting temperature (T_m) were determined by differential scanning calorimetry (DSC). The detailed discussion regarding composition optimization, synthesis techniques, XRD, and DSC have been reported elsewhere [25].

The corrosion behavior of the $Hf_{64}Cu_{18}Ni_{18}$ ribbon was investigated by potentiodynamic polarization techniques and electrochemical impedance spectroscopy (EIS). The ribbon was polished to make the uniform surface finish. Further, it was cleaned with acetone and dried in air. HCl and NaOH electrolyte solutions were used to investigate corrosion behavior, with 0.05, 0.1, and 0.5 molar solutions. These solutions were prepared from reagent grade

chemicals and double-distilled water. The corrosion test was performed at room temperature using three-electrode system. The platinum was used as the counter-electrode, whereas saturated calomel electrode (SCE, 241 mV_{SHE}) was used as a reference electrode. Polarization plot was obtained from the Biologic SP-150 potentiostat instrument with the scan rate of 0.167 mV/s. The working electrode was immersed in the solution and subjected to the area of 0.5 cm^2 while the other surface of ribbon adhesive with Araldite to ensure the electrical isolation. The sample achieved stable open-circuit potentials (OCP) after 30 min in all the experiments. The EIS measurements were taken in the frequency range of 10 Hz to 100 MHz at the OCP. Each experiment was conducted with a new electrolyte solution of 200 ml. Electrochemical corrosion kinetics parameters such as corrosion current density (i_{corr}) and corrosion potential (E_{corr}) were determined by applying the Tafel extrapolation method in EC-Lab V10.37 software [26]. The surface morphology of the ribbon after the polarization test was examined by scanning electron microscope (SEM, JEOL JSM-6380A) coupled with energy-dispersive spectroscopy (EDS) for the compositional analysis.

3 Results and Discussion

3.1 Corrosion Behavior of $Hf_{64}Cu_{18}Ni_{18}$ MG in NaOH Electrolyte

3.1.1 Potentiodynamic Polarization

The potentiodynamic polarization curve of the $Hf_{64}Cu_{18}Ni_{18}$ glassy ribbon in NaOH solution with different
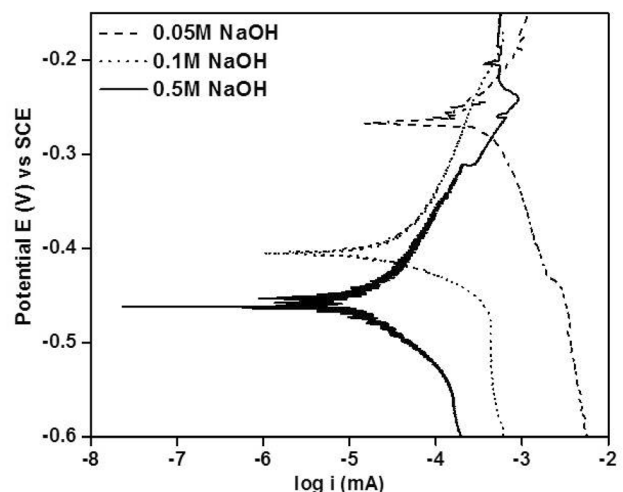
Fig.1 Polarization curve of $Hf_{64}Cu_{18}Ni_{18}$ metallic glass in NaOH solution

concentrations is shown in Fig. 1. The MG ribbon shows the dissolution state in the anodic region in all the molar concentrations. Dissolution is electrochemical process in which MG ribbon is dissolved from the work piece and gases are liberated at the surface. From Fig. 1, it can be confirmed that the polarization curve follows small passivation up to the potential of − 150 mV except 0.05 M NaOH solution. This potential corresponds to the maximum potential used in the present experiments. The corrosion current density (i_{corr}) and corrosion potential (E_{corr}) of MG extracted from the polarization curve by Tafel extrapolation are listed in Table 1. It is observed that the E_{corr} shifts significantly toward the more negative side when NaOH concentration increases from 0.05 to 0.5 M. This variation may be due to potential scanning rate [27], surface finish of the sample [10], the aeration conditions of the electrolyte [28], and the geometry of sample. The potential scanning rate and the geometry of the sample are same in all the experiment. Hence, the shifting in E_{corr} has been observed due to the surface finish of the sample. The MG ribbon produced by rapid solidification processing is homogeneous in nature without any second-phase particle. Still due to the differential thermal gradient, there might be some discontinuity on the solidified ribbon [12]. These discontinuities create roughness on the surface causing the shift in E_{corr} during potentiodynamic polarization measurements. However, it has also been noticed that the corrosion current density (i_{corr}) of MG ribbon decreases for the higher molar concentration of NaOH (0.1 and 0.5 M). It is observed from Table 1 that the i_{corr} values decrease from 0.19 to 0.06 µA/cm^2 with the increase in concentration of NaOH from 0.1 to 0.5 M, respectively. Based on i_{corr} value, it can be concluded that 0.5 M NaOH has good corrosion resistance than 0.05 M and 0.1 M. This is due to the availability of OH^- ions to stabilize the passivity [29, 30]. As the passive layer becomes stable due to OH^- ions, the corrosion resistance increases in 0.5 M NaOH compared to the other molar solutions. Passive layer stability due to OH^- ions has already been reported earlier [29, 30]. Gebert et al. [29] reported the corrosion behavior of $Mg_{65}Y_{10}Cu_{15}Ag_{10}$ amorphous sample and concluded that passive layer formed in alkaline electrolyte is thinner in nature due to the formation of magnesium and yttrium oxide/hydroxides. Lekatou et al. [30] investigated the

corrosion behavior of Fe-40Ni-20B (at.%) metal glasses and reported the stability of passive layer due to the formation of active and passive corrosion product. Active corrosion product consists of α-$Ni(OH)_2$, NiO, and $Ni(OH)_2$-2NiOOH whereas passive corrosion product includes phases such as NiO, β-NiOOH. Fe_2O_3. Fe_3O_4, and α-FeOOH. In the present investigation, it can be concluded that hafnium oxide or hydroxides might be the corrosion product in NaOH solution and increases with its concentration. The evidence of hafnium oxide formation has been addressed in the subsequent chapter.

3.1.2 Electrochemical Impedance Spectroscopy (EIS)

Electrochemical impedance spectroscopy (EIS) is one of the most versatile techniques to determine the corrosion behavior of the metallic alloys. It measures the resistance of electrode and electrode-solution interfaces by predicting the structure of the passive layer of the materials [18, 31]. The impedance results (Nyquist plot) of $Hf_{64}Cu_{18}Ni_{18}$ MG in NaOH solution with different concentrations are shown in Fig. 2. It is well known that the diameter of the semicircle of the Nyquist plot is a good indicator of passivity of alloy and its resistance to corrosion [32]. 0.5 M NaOH solution shows a larger capacitive loop diameter than the 0.05 and 0.1 M NaOH. To further understand the EIS of MG, the obtained curves are fitted using the electrical circuit analogy. The fitted model can be represented in the form of an equivalent circuit diagram, as shown in Fig. 2. The model consists of one capacitance (Q_1) and two resistances (R_s and R_p). Here Q_1 is the constant phase element corresponding to the capacitance of passive layer formation. The R_s and R_p are solution resistance and film resistance of the corrosion process on the metal surface (polarization resistance), respectively. The mathematical formula for the electrical circuit is expressed as $R_s + (\frac{Q_1}{R_p})$. In all cases, the quality of the fitting is adjusted by chi-square (χ^2) in EC-Lab V10.37 software. The polarization resistance (R_p) of 0.05 M NaOH is 44375 Ω cm^2 and shows the smaller semicircle diameter indicating poor corrosion resistance. The EIS parameters R_s and R_p are mentioned in Table 2. The Nyquist plot diameter and polarization resistance increase with the concentration of solutions, indicating the improvement in corrosion resistance of MG.

Table 1 Corrosion current density (i_{corr}) and corrosion potential (E_{corr}) of $Hf_{64}Cu_{18}Ni_{18}$ MG ribbon obtained from polarization curve

Solution	NaOH			HCl		
Molarity	0.05	0.1	0.5	0.05	0.1	0.5
E_{corr} (mV vs. SCE)	− 272	− 283	− 388	− 368	− 247	− 327
i_{corr} (µA/cm^2)	0.40	0.19	0.06	0.68	2.45	2.75

Fig.2 Impedance spectra and equivalent circuit of $Hf_{64}Cu_{18}Ni_{18}$ metallic glass in NaOH solution
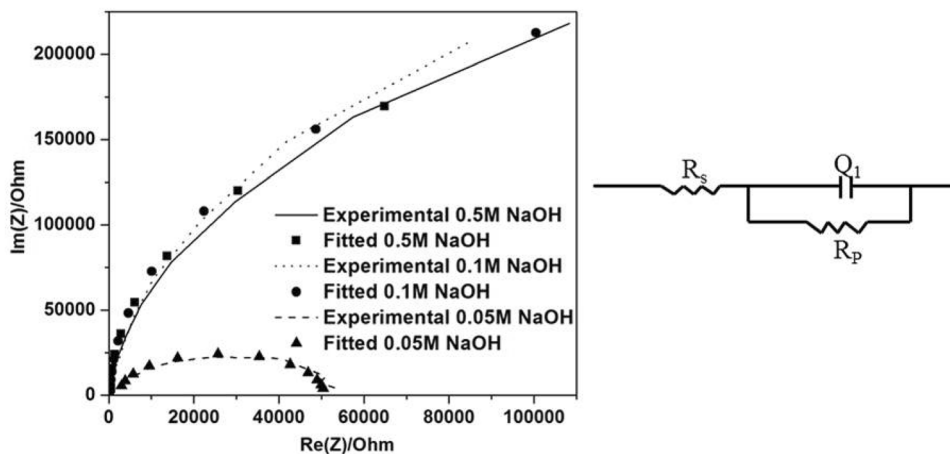


Table 2 Solution resistance (R_s) and polarization resistance (R_p), of $Hf_{64}Cu_{18}Ni_{18}$ MG ribbon in NaOH solution

Molarity	0.05	0.1	0.5
R_s (Ohm cm^2) Solution resistance	546	96	93
R_p (Ohm cm^2) Polarization resistance	44,375	389,162	464,996

Therefore, it can be concluded that MG in 0.5 M NaOH solution has the good corrosion resistance in the present study. This shows that the impedance spectroscopy and polarization results are consistent with each other in alkaline solution.

3.1.3 Corrosion Product Characterization by SEM and EDS

In the present investigation, SEM was carried out to observe surface morphology after the polarization test. The morphology of the as-cast ribbon sample is shown in Fig. 3
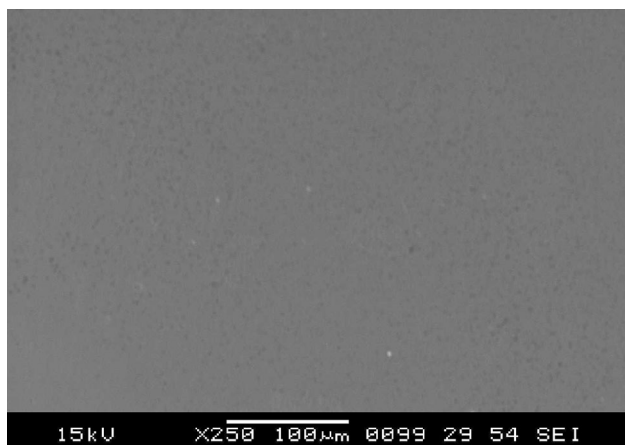
Fig.3 SEM morphology of as-cast $Hf_{64}Cu_{18}Ni_{18}$ metallic glass

to compare the corroded surface after the polarization test. The similar nature of the corroded surface of glassy ribbon has been observed in different concentration of NaOH solutions. It can be seen from Fig. 4 that the area of the corroded surface decreases with the concentration of the solution. The morphology of corroded surface looks like grooves, scratches, and decreases with the increase in NaOH concentration. The formation of grooves and scratches is attributed to defects and inclusions present in the ribbon. Figure 4a shows the scratched surface; the intensity of scratches decreases with the increase in concentration. This again confirms that the ribbon sample possesses good corrosion resistances in 0.5 M NaOH solution. This concludes that the polarization and SEM results are corresponding to each other. Furthermore, EDS analysis has also been done to determine the elements present in the grooves. All the elemental composition, including oxygen, is mentioned in Table 3. The EDS result reveals that oxygen (O) and hafnium (Hf) have a maximum concentration in the corroded surface, whereas on the glassy surface of Hf, Cu, and Ni are more. Hf has a strong tendency toward oxidization. Moreover, the presence of hydroxide ions makes Hf more favorable to form oxides [29, 30]. Therefore, it can be concluded that HfO_2 is formed as a corrosion product during the polarization test.
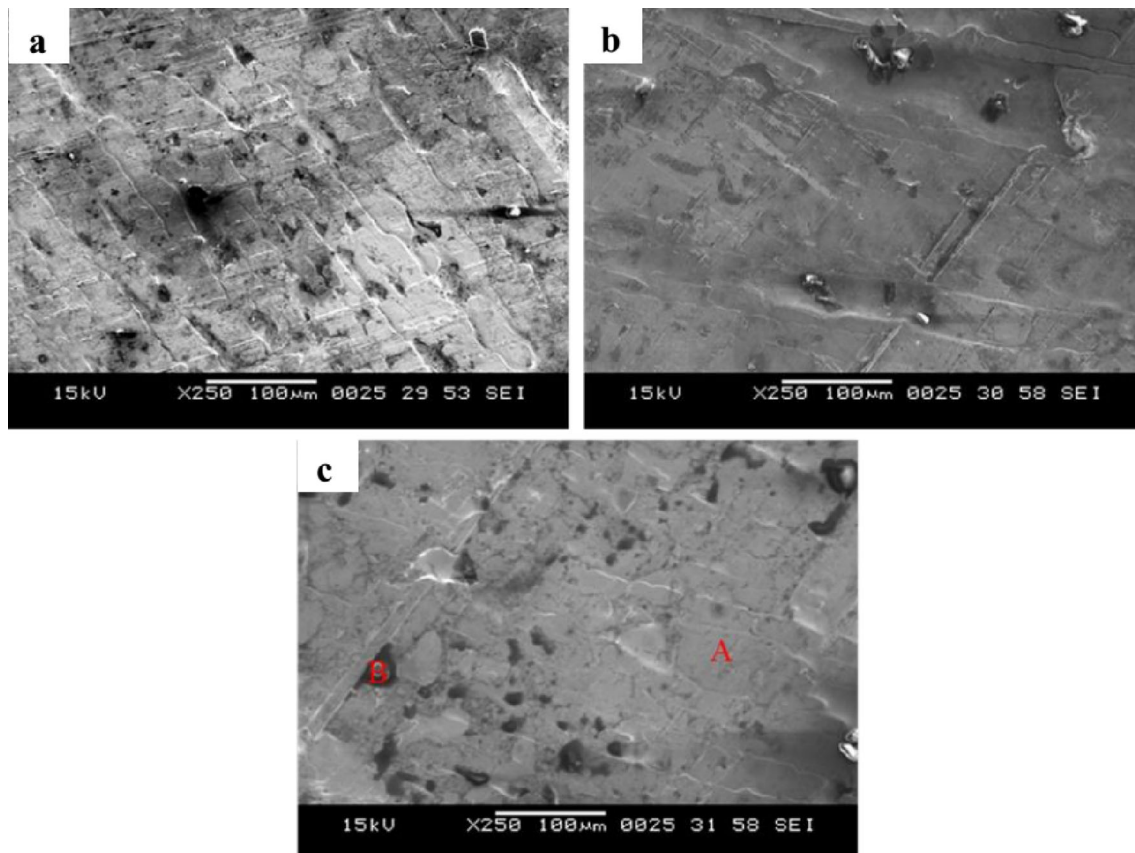
Fig.4 SEM micrograph of $Hf_{64}Cu_{18}Ni_{18}$ metallic glass corroded in **a** 0.05, **b** 0.1, **c** 0.5 M NaOH solution

Table 3 Content of the alloying element obtained from the EDS in 0.5 M NaOH and HCl solution of $Hf_{64}Cu_{18}Ni_{18}$ metallic glass ribbon

| Elements (at %)	NaOH		HCl	
	Surface (A)	Grooves (B)	Surface (A)	Pits (B)
Hf	55.47	13.97	52.47	32.18
Cu	13.45	5.00	13.08	7.33
Ni	17.15	5.03	15.39	3.74
Na	2.89	4.97	–	–
O	10.95	71.04	19.07	56.75

3.2 Corrosion Behavior of $Hf_{64}Cu_{18}Ni_{18}$ MG in HCl Electrolyte

3.2.1 Potentiodynamic Polarization

Figure 5 illustrates the $Hf_{64}Cu_{18}Ni_{18}$ MG ribbon's polarization curve in an aqueous HCl solution with different concentration. Passivation has not been observed in all the molar solutions, as shown in Fig. 5. E_{corr} and i_{corr} values obtained from the polarization curve are shown in Table 1. It has been observed that i_{corr} values increase from 2.45 to 2.75 $\mu A/cm^2$ when the HCl concentration is increased from 0.1 to 0.5 M, respectively. This behavior suggests the reduction in corrosion resistance of ribbon with the concentration of HCl. It is well known that chloride ions are the most common aggressive corrosive media. Thus, as the concentration of the solution increases, the i_{corr} value increases too, resulting in the degradation of the ribbon sample. Due to the degradation of the ribbon sample in 0.5 M HCl solution, the maximum number of spherical pits has been observed in the SEM. Similar kind of results has also been reported in most of the glassy systems [33]. The SEM results and the reasons for the formation of the pits have been discussed in the subsequent section.
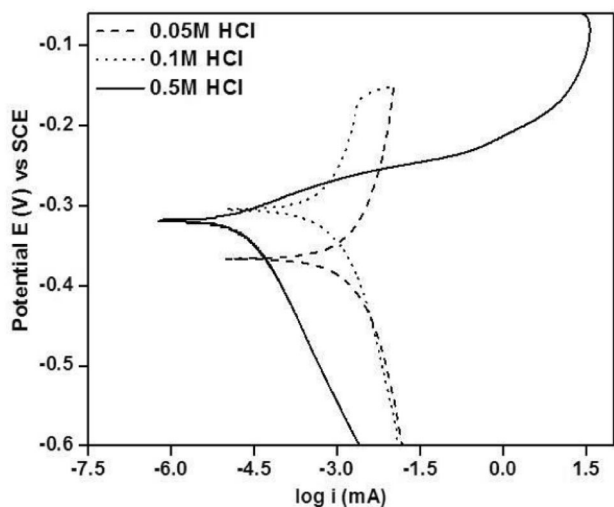
Fig.5 Polarization curve of $Hf_{64}Cu_{18}Ni_{18}$ metallic glass in HCl solution

3.2.2 Corrosion Product Characterization by SEM and EDS

The corroded surface morphology of $Hf_{64}Cu_{18}Ni_{18}$ MG in the HCl solution has also been investigated and is shown in Fig. 6. It can be observed from Fig. 6 that MG corrodes in

all the three molar solutions, namely 0.05, 0.1, and 0.5. The corrosion of MG is initiated in the 0.05 M solution (Fig. 6a) and shows the ridges formation. As the chloride concentration increases, it results in a larger ridge on the surface, as shown in Fig. 6b. Further increase in the concentration of chloride ions to 0.5 M results in the ridge break down. The acidic solution gradually drips into it, indicating the pit formation, as shown in Fig. 6c. These results are consistent with the polarization curve, as shown in Fig. 5. The pits developed look like spherical structures and spread across the sample surface. The reason for the formation of the pit may be as follows. The MGs are generally considered as chemically homogeneous materials without any secondary phase, inclusions, and defects. However, during the melt spinning process, occurrences of these defects due to differential cooling gradient cannot be completely neglected [13]. Earlier reports have shown Zr-based [11] and Cu-based [14] MGs are more prone to pitting corrosion. These pits are initiated at the interfaces between such defects and surrounding amorphous matrix [7, 10, 34]. The chloride ions will preferentially be absorbed in these inclusions and defects when the sample is immersed in an electrolyte solution and forms the galvanic couples among these defects and surrounding matrix [13]. Hence, these inclusions and defects act as energetically
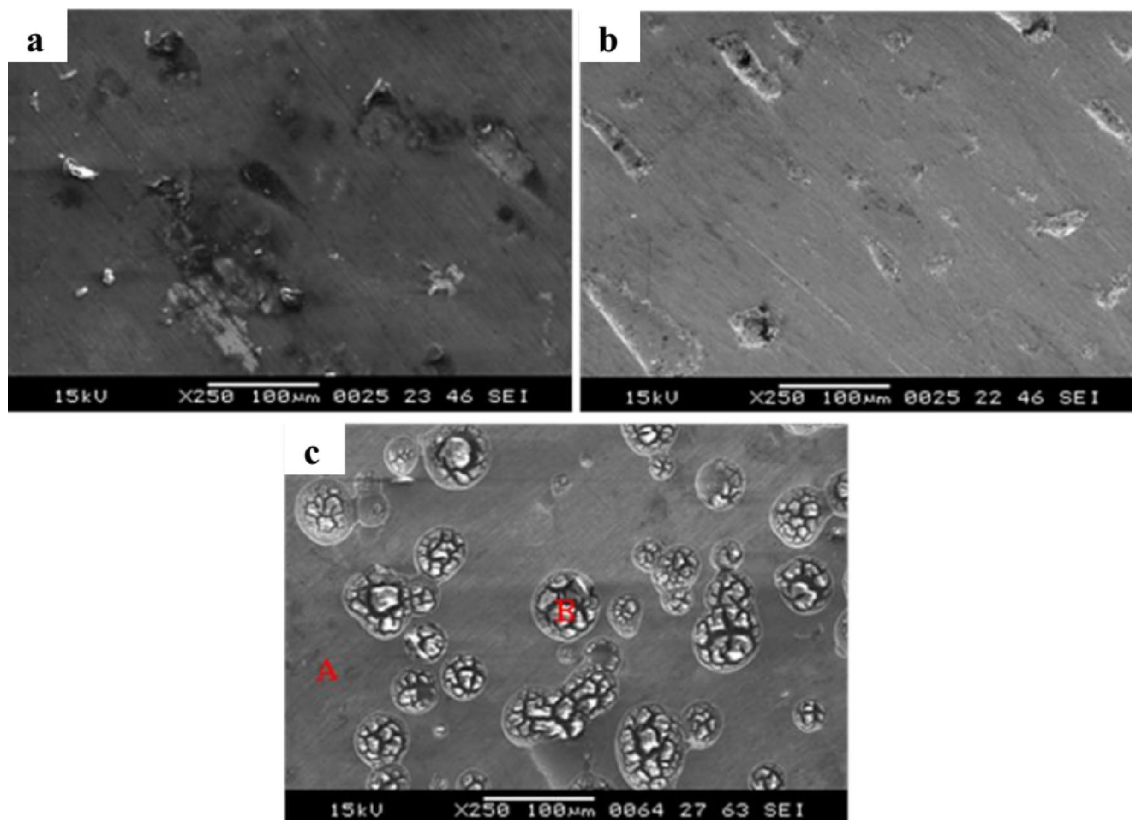
Fig.6 SEM micrograph of $Hf_{64}Cu_{18}Ni_{18}$ metallic glass corroded in **a** 0.05, **b** 0.1, **c** 0.5 M HCl solution

favorable sites to corrode the sample. Green et al.[35] and Gebert et al. [9] reported the pit initiation and growth mechanism in which selective dissolution of participating elements takes place at the sites of chemical and physical defects on the BMG surface, which leads to pitting corrosion. The other reason may be the selective dissolution of Hf or the simultaneous dissolution of Hf, Cu, and Ni [36]. It is well established that the Cu is a nobler element than Hf and Ni; the standard electrode potentials for Hf/Hf^{4+}, Ni/Ni^{2+}, and Cu/Cu^{2+} couples are -1.70 V_{SHE}, -0.25 $V_{SHE,}$ and 0.34 V_{SHE}, respectively [26]. The significant equilibrium electrode potential difference between Cu-Ni and Cu-Hf can produce enough potential for selective dissolution of Hf and Ni in Hf-Cu-Ni MG, which further results in HfO_2 and NiO formation on the surface. Hf being less-nobler metal, the selective dissolution of Hf is possible due to the difference in electrode potential. In the present investigation, it has been anticipated that HfO_2 would form on the surface due to higher Hf concentration and its strong affinity toward oxide formation. Table 3 indicates the content of alloying elements on the surface and the pits of 0.5 M HCl solution. The EDS results confirm that pits contain a higher amount of oxygen (O) and hafnium (Hf). Hf and O amount in the pits are found as 32.18 and 56.75 at. %. According to stoichiometric analysis, it can be concluded that HfO_2 is formed as a corrosion product in the pits. Moreover, the EDS line scan analysis has also been done to identify the elements present in pits. The line scan of the glassy ribbon corroded in 0.5 M HCl is shown in Fig. 7. All the elements show the non-uniform line profile across the corroded surface. The intensity of the elements has been found to be in the order of O > Hf > Cu > Ni in the pits, whereas on the surface it follows Hf > Cu > Ni > O. This indicates that the Hf atoms diffuse in the pits followed by Cu and Ni. The investigated glassy ribbon content is 64at% of Hf. Moreover, it has strong tendency toward oxidization, confirming the formation of HfO_2 in the pits. Hence, from the EDS data and line scan analysis, it can be concluded that HfO_2 forms in the pits as corrosion products.

4 Conclusion

The influence of acidic and alkaline attacks on corrosion behavior of $Hf_{64}Cu_{18}Ni_{18}$ MG ribbon has been studied, and the results are summarized as follows.

1. The MG ribbon possesses good corrosion resistance in NaOH than HCl. The presence of hydroxides ions is the primary reason for passivation on the surface.

2. The corroded surface appears like grooves and scratches in NaOH solution, while in HCl, spherical pits are formed.

3. Corrosion product HfO_2 is formed on the surface in NaOH and HCl solutions due to the strong oxidation tendency of Hf.

Fig.7 EDS line scan of $Hf_{64}Cu_{18}Ni_{18}$ metallic glass corroded in 0.5 M HCl solution and at the bottom green line indicates the location of the scan
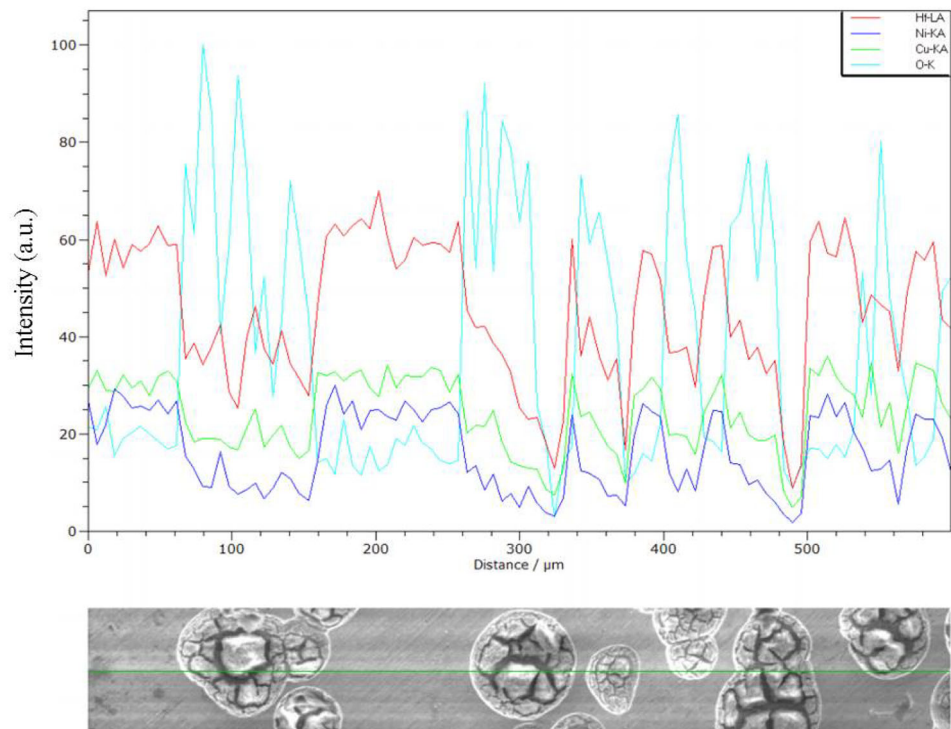
References

[1] Wang W H, Dong C, and Shek C H, *Mater Sci Eng R* 44 (2004) 45.

[2] Suryanarayana C, *Non-equilibrium processing of material*, Oxford, U.K. Pergamon, (1999) p 318.

[3] Greer A L, Cheng Y Q, and Ma E, *Mat Sci Eng R* 74 (2013) 71.

[4] Yavari A R, Lewandowski J J, and Eckert J, *MRS Bull* 32 (2007) 635.

[5] Suryanarayana C,and Inoue A, *Bulk Metallic glasses*, CRC Press, Boca Raton, FL, (2001) p 481.

[6] Zander D, Heisterkamp B, and Gallino I, *J. Alloys Compd* 434-435 (2007) 234.

[7] Gostin P F, Gebert A, and Schultz L, *Corros Sci* 52 (2010) 273–281.

[8] Wang Z M, Zhang J, Chang X C, Hou W L, and Wang J Q, *Corros Sci* 52 (2010) 1342.

[9] Gebert A, Gostin P F, and Schultz L, *Corros Sci* 52 (2010) 1711.

[10] Lu H B, Li Y, and Wang F H, *Corros Sci* 48 (2006) 2106.

[11] Kawashima A, Ohmura K, Yokoyama Y, and Inoue A, *Corros Sci* 53 (2011) 2778.

[12] Si J J, Chen X H, Cai Y H, Wu Y D, Wang T, and Hui X H, *Corros Sci* 107 (2016) 123.

[13] Cai A H, Xiong X, Liu Y, An W K, Zhou G J, Luo Y, and Li T L, *Mater Chem Phys* 134 (2012) 938.

[14] Lin H M, Wu J K, Wang C C, and Lee P Y, *Mater Lett* 62 (2008) 2995.

[15] Babilas R, Bajorek A, Simka W, and Babilas D, *Electrochim Acta* 209 (2016) 632.

[16] Gebert A, Haehnel V, Park E S, Kim D H, and Schultz L, *Electrochim Acta* 53 (2008) 3403

[17] Chlewicka M, Cieslak G, and Mizera J, *Mater Corros* 70 (2019) 2073.

[18] Huang C H, Lai J J, Huang J C, Lin C H, and Jang J S C, *Mater Sci Eng C* 62 (2016) 368.

[19] Li G, Huang L, Dong Y G, He G W, Qi L, Jing Q, Ma M Z, and Liu R P, *Sci China Phys Mech Astron* 53 (2010) 435.

[20] Chattoraj I, Baunack S, Stoica M, and Gebert A, *Mater Corros* 55 (2004) 36.

[21] Li C, Wang L, and Inoue A, *Mater Lett* 51 (2001) 203.

[22] Louzguine D V, Ko M S, Ranganathan S, and Inoue A, *J. Nanosci. and Nanotech* 1 (2001) 185.

[23] Zhang T, Inoue A, and Masumoto T, *Mater Sci Engg A* 182 (1994) 1423.

[24] Cui Y Y, Bai X, Luo S Y, Wang Q, Li J H, and Liu B X, *J. Alloys Compd* 552 (2013) 55.

[25] Khond A, Babu D A, Smaran S, Deshmukh A, Majumdar B, Bhatt J, and Srivastav A K, *J Non-Cryst Solids* 500 (2018) 191.

[26] Corrosion, *ASM Metals Handbook*, Volume 13, 1980 p 16.

[27] Manning P E, *Corrosion* 36 (1980) 468.

[28] Barbosa M A, Garrido A, Campilho A, and Sutherland I, *Corros Sci* 32 (1991) 179.

[29] Gebert A, Subba Rao R V, Wolff U, Baunack S, Eckert J, and Schultz L, *Mater Sci Eng A* 375-377 (2004) 280.

[30] Lekatou A, Marinou A, Patsalas P, and Karakassides M A, *J Alloys Compd* 483 (2009) 514.

[31] Wang Y B, Zheng Y F, Wei S C, and Li M, *J Biomed Mater Res* 96 (2011) 34.

[32] Elkin V V, Marshakov A I, Rybkina A A, and Maleeva M A, *Russ J Electrochem* 47 (2011) 136.

[33] Scully J R, Gebert A, and Payer J H, *J Mater Res* 22 (2007) 302.

[34] Gebert A, Kuehn U, Baunack S, Mattern N, and Schultz L, *Mater Sci Eng A* 415 (2006) 242.

[35] Green B A, Meyer H M, Benson R S, Yokoyama Y, Liaw P K, and Liu C T, *Corros Sci* 50 (2008) 1825.

[36] Mandal S, Sivakumar B, Singhbabu Y N, Bandyopadhyay N R, Chattopadhyay P P, and Kailath A J, *J Mater Eng Perform* 1059 (2019) 1.